

Ubiquitin-immunoreactive degradation products of cytokeratin 8/18 correlate with aggressive breast cancer

Keiichi Iwaya,¹ Hitoshi Ogawa,¹ Yasuo Mukai,¹ Akihiro Iwamatsu² and Kiyoshi Mukai^{1, 3}

¹Department of Pathology, Tokyo Medical University, 6-1-1 Shinjuku, Shinjuku-ku, Tokyo 160-8402; and ²Central Laboratories for Key Technology, Kirin Brewery Co., Ltd., 1-13-5 Fukuura, Kanazawa-ku, Yokohama-shi, Kanagawa 236-0004

(Received April 7, 2003/Revised August 4, 2003/Accepted August 11, 2003)

Decreased amounts of cytokeratin (CK) 8/18 in the cytoplasm of breast cancer cells correlate with a poor prognosis. Although such decreases have been attributed to suppressed gene expression, accelerated protein degradation may also be responsible. In order to investigate whether selective degradation via the ubiquitin (Ub)-dependent proteasome pathway occurs in breast cancer, one- and two-dimensional (1-D and 2-D) immunoblot analysis was performed on cancerous and normal breast tissue from 50 breast cancer patients using the anti-Ub monoclonal antibodies (mAbs) KM691 and KM690. On 1-D gel electrophoresis, one broad band or two bands were detected at about 43 kDa; these were detected only in cancer tissue. Immunoreactive bands at 43 kDa were significantly associated with aggressive morphology ($P=0.011$), nuclear p53 accumulation ($P=0.015$) and overexpression of Her2/*neu* protein ($P=0.012$). On 2-D gel electrophoresis, these bands were fractionated into a group of several spots that formed a staircase pattern at 40–45 kDa. Partial amino acid sequencing analysis demonstrated that these Ub-immunoreactive spots corresponded to CK8 and CK18; however, since they did not have an amino-terminal domain, and were located at lower molecular weight positions than intact CK8 and CK18 on the 2-D gel, they were regarded as degradation products. CK18 degradation was confirmed by confocal microscopy as loss of the frame-like network that forms the luminal structure. These results indicate that CK 8/18 degradation products are detected specifically in breast cancer and may determine its aggressiveness. (*Cancer Sci* 2003; 94: 864–870)

Ubiquitin (Ub) is present in all eukaryotic cells and is one of the most highly conserved proteins known.^{1,2} It can exist either in its free form or be covalently bound to a variety of cytoplasmic, nuclear and integral membrane proteins, and is essential for the selective degradation of these proteins.^{3,4} Recent biochemical and genetic evidence has indicated that Ub conjugation leads to selective degradation of nuclear oncoproteins and suppressor gene products.^{5,6} Furthermore, immunohistochemical studies with anti-Ub monoclonal antibodies (mAbs) have demonstrated strong staining in the majority of malignant tumors, suggesting that Ub-dependent proteolysis is accelerated in the neoplastic state.^{7,8}

One line of evidence that Ub-dependent proteolysis is involved in neoplastic transformation is the nuclear accumulation of p53 protein. In normal cells, p53 protein is present in such small amounts, and for such a short time during the late G1 phase (its half-life is only 6 to 30 min), that it cannot be detected by ordinary immunohistochemical techniques, even in actively dividing cells. In contrast, accumulation of mutated p53 is apparent in the nuclei of various types of human cancer cells, where it impairs the regulation of many transcriptional factors and endows the cells with oncogenic activity.^{9–12} Immunohistochemical detection of p53 in the nuclei of breast cancer

cells is associated with a poor prognosis, which is consistent with rapid progression.^{13,14} Moreover, several studies have reported that nuclear accumulation of p53 correlates with high histologic grade.^{15,16} Our previous study of breast cancer tissue, however, suggested that the formation of a p53-heat shock protein (hsp) 70 complex is not the major mechanism of p53 stabilization, and that the Ub-dependent pathway may be responsible for maintaining steady-state levels of p53 protein.¹⁷ The Ub-dependent degradation pathway has also been shown to be involved in the turnover of p53 by others.^{18,19}

Following our earlier results,¹⁷ we were interested in determining whether increased Ub-dependent proteolysis shortens the half-lives of other cellular proteins, thereby causing a reorganization of the cellular structure which would in turn contribute to the characteristics of the cancerous state. Therefore, in the present study, we used two-dimensional (2-D) polyacrylamide gel electrophoresis (PAGE) followed by immunoblot analysis with anti-Ub mAbs, together with sequencing analysis, in an attempt to identify tumor-specific Ub-conjugated proteins in breast cancer tissue.

Materials and Methods

Tumor tissue. We investigated a total of 50 primary breast cancer specimens obtained during resection at Tokyo Medical University Hospital between 1998 and 1999. Cancerous and normal breast tissues taken from the same specimen were divided into four parts: one was formalin-fixed and paraffin-embedded for routine histopathological diagnosis, another was fresh-frozen for one-dimensional (1-D) and 2-D PAGE followed by immunoblotting, immunoprecipitation, and amino acid sequencing, the third was processed by the acetone-methyl benzoate-xylene (AmeX) method²⁰ to produce acetone-fixed, paraffin-embedded tissue for an immunohistochemical study of p53 and cytokeratin (CK) 18, and the fourth was fixed with 4% paraformaldehyde for about 24 h before embedding in paraffin for an immunohistochemical assessment of estrogen receptor (ER) and progesterone receptor (PgR) status, and of Her2/*neu* protein. Histologic grading of the primary tumor was performed according to a system based on a modification of the World Health Organization (WHO) classification.²¹

The 50 patients from whom the surgical specimens were obtained ranged in age from 31 to 79 years (mean, 54.4 years) and had undergone modified radical or partial mastectomy. The largest dimensions of the tumors ranged from 1.3 to 10 cm. Signed informed consent to use their specimens was obtained from each patient according to the institutional guidelines.

Immunoblot analysis. Breast cancer and normal breast tissue from the same specimen were separated and minced on ice with plastic surgical scissors. Approximately 200 mg of tissue was suspended in 1 ml of lysis buffer composed of 1% sodium

³To whom correspondence should be addressed. E-mail: kmukai@tokyo-med.ac.jp

dodecyl sulfate (SDS) buffer containing Tris-HCl (pH 8.8), 1 mM ethylenediaminetetraacetate (EDTA) and 10 mM dithiothreitol. The extract was homogenized in a Polytron homogenizer, and fresh N-ethylmaleimide was added as an inhibitor of endogenous Ub isopeptidases. The preparations were extracted by vigorous sonification (Handy sonic, model UR-20P, Tomy Seiko Co., Ltd., Tokyo) in this buffer. After centrifugation at 13,000g for 10 min at 4°C, 5 µl of the supernatant was mixed with the same volume of Laemmli solution (2% SDS, 10% glycerol, 100 mM dithiothreitol, 60 mM Tris buffer [pH 6.8] and 0.001% bromophenol blue) and denatured for 5 min at 100°C. Samples of the breast cancer and normal breast tissue preparations were applied alternately to 10% SDS-4% polyacrylamide stacking gel. The residual pellet was saturated with urea and dissolved by vigorous shaking at room temperature for 10 min. After centrifugation at 10,000g for 5 min, the protein concentration of the supernatant was measured using Bradford's method.²² For 2-D PAGE, 200 µg of the supernatant was loaded on a Protean II xi multi-cell electrophoresis apparatus ("The Proteome Works" system, Bio-Rad, Hercules, CA). Pre-cast pH 5–7 immobilized gradient strips were used as the first dimension and 10% polyacrylamide gel as the second dimension.

After 1-D or 2-D SDS-PAGE, the fractionated proteins were transferred onto polyvinylidene difluoride (PVDF) membranes (Immobilon-P, Millipore, Bedford, MA) in a transfer buffer consisting of 25 mM Tris buffer, 192 mM glycine, 20% methanol and 0.1% SDS. Two primary mAbs against human Ub, KM691 and KM680, produced in mouse hybridoma cells by a standard method, were used for the immunoblot analysis.²³ The specificity of KM691 and KM680 was confirmed by their specific reaction against Ub in a Ub-protein ligation system containing E1, E2 and E3,²⁴ which were kindly provided by Dr. Keiji Tanaka, Department of Molecular Oncology, Tokyo Metropolitan Institute of Medical Science. The immunoblotting procedure was as follows: (1) incubation for 3 h with a blocking buffer consisting of 5% skim milk and 1% bovine serum albumin dissolved in phosphate-buffered saline (PBS); (2) incubation overnight at 4°C with the primary mAb; (3) washing three times with 0.1% Tween-20 in PBS; (4) incubation for 30 min with peroxidase-conjugated anti-mouse IgG (Immuno-Biological Labs., Fujioka), diluted to 1/1000; (5) washing three times with 0.1% Tween-20 in PBS; and (6) incubation with enhanced chemiluminescence reagents (ECL, Amersham, Buckinghamshire, UK) to develop a colored product, and recording using a gel documentation system (Gel Doc II, Bio-Rad).

Purification of proteins from the 2-D gels and *in situ* protein digestion on PVDF. The proteins were fractionated by 2-D PAGE using the same apparatus, sample preparation method and first and second gel compositions as described above. The gel was stained with 0.3 M CuCl₂ for 5 min and washed twice with water (for 5 min each time). After photographing the gel with X-ray film (XAR-5, Kodak, Rochester, NY), the protein spots were destained, blotted onto a PVDF membrane (Immobilon-PSQ, Millipore) with Tris-aminocaproic acid-methanol buffer, visualized by staining with 0.1% Ponceau S in 1% acetic acid for 5 min, and washed three times with water.

Guided by both the films of the CuCl₂-stained gels and the immunoblots, the target protein spots were cut out with a clean razor and transferred to Eppendorf tubes (1.5 ml). Several spots on the nitrocellulose membranes were destained by washing with 200 mM NaOH for 1–2 min and with distilled water, then suspended in 500 µl of reducing solution comprising 6 M guanidine, 0.5 M Tris buffer (pH 8.6), 0.3% EDTA, 2% acetonitrile and 1 mg of dithiothreitol at 60°C. One hour later, 2.4 mg of iodoacetic acid dissolved in 10 µl of 0.5 M NaOH was added to the reducing solution, and S-carboxymethylation was allowed to continue for 15–20 min in the dark, with stirring.²⁵

The membrane was thoroughly washed with 2% acetonitrile, then stirred in 0.1% SDS for 5 min. In order to prevent protease adsorption on the PVDF membrane, the blots were incubated with 1 ml of 0.5% polyvinylpyrrolidone 40 in 100 mM acetic acid for 20 min at room temperature and rinsed vigorously with the digestion buffer. *In situ* digestion was performed using *Achromobacter* protease I (Wako, Osaka) at an enzyme-to-substrate ratio of 1:100 (mol/mol) in reaction buffer (90 mM Tris buffer [pH 9.0] and 8% acetonitrile) for 16 h at 30°C.²⁶

Reverse-phase high-performance liquid chromatography (HPLC) peptide mapping and sequencing. After *in situ* digestion, the supernatant was removed, diluted with water, injected into a µ-Bondasphere 5 µC8-300Å column (2.1×150 mm, Waters, Milford, MA) and subjected to HPLC on a Hitachi L6200/6000 liquid chromatograph (Hitachi, Tokyo). The peptides were eluted with a linear gradient of 2–50% solvent B (0.02% trifluoroacetic acid in 2-propanol: acetonitrile, 7:3 [v/v]) using solvent A (0.05% trifluoroacetic acid) at a flow rate of 0.25 ml, and fractionated manually by monitoring the absorbance at 214 nm with a Hitachi L4000 detector (Hitachi). Amino acid sequencing was then performed on a Shimadzu PSQ-1 sequencer (Shimadzu, Kyoto) or a 470A Applied Biosystems sequencer (ABI Japan, Tokyo). The phenylthiohydrated amino acids thus obtained were identified by isometric HPLC for amino acid sequencing and mass spectrometric analysis.

Molecular weight determination and protein identification. Molecular weight determination was carried out on a Sciex API-III mass spectrometer (ABI Japan) fitted with an ion-spray (pneumatically assisted electrospray) interface and a quadrupole mass analyzer with an upper mass limit of $m/z=2400$ Da. On-line liquid chromatography/mass spectrometry was performed using an Inertsil ODS-2 column 5 µm (0.5×60 mm; GL Science, Tokyo). The peptides were eluted with a linear gradient of solvent B in 30 min at a flow rate of 5 µl/min using the following solutions: solvent A (0.1% trifluoroacetic acid in water) and solvent B (0.1% trifluoroacetic acid in 2-propanol: acetonitrile, 7:3 [v/v]).

The proteins were identified by searching a protein sequence database (National Center for Biotechnology Information, Bethesda, MD) and comparing the masses determined with the theoretical masses of the *Achromobacter* protease I-digested fragments, as previously described.²⁷

Immunoprecipitation of Ub-immunoreactive CK8/18. Extracts from breast cancer tissue and normal breast tissue of the same specimen were prepared by the same method using the same lysis buffer for immunoblot analysis described above. Extracts were immunoprecipitated with anti-Ub rabbit polyclonal antibody which had been raised by injection of bovine red cell Ub coupled with bovine serum albumin.²⁴ The immunoprecipitation was performed as previously described.¹⁷ The precipitated samples were immunoblotted with anti-CK18 mouse monoclonal antibody (DC10, DAKO Cytomation California, Inc., Carpinteria, CA), diluted to 1/200. Then immunoprecipitation of the same extracts was performed with anti-CK8/18 pig polyclonal antibody (PROGEN Biotechnik GmbH, Heidelberg, Germany). Ub-conjugated proteins in the precipitated sample were detected by immunoblot analysis using KM691.

Immunohistochemistry and confocal microscopy. The AmEx blocks of the breast cancer tissue were cut into 3-µm-thick sections, deparaffinized and incubated for 1 h with a mouse anti-CK18 mAb (DC10, Dako Japan, Kyoto) diluted to 1:80. An Alexa Fluor488-labelled anti-mouse mAb (dilution 1:200; Molecular Probes, Inc., Eugene, OR) was used as a secondary antibody, and the nuclei were counterstained with Hoechst Dye 33258 trihydrochloride (Dojindo, Kumamoto). Confocal microscopy was performed using a Bio-Rad Radiance 2000 confocal scanning laser microscope (Bio-Rad, Hemel Hempstead, UK).

Immunostaining for p53 and Her2/*neu* protein was performed according to a previously described procedure.¹⁶⁾ The specimen was judged to be p53-positive when more than 10% of the nuclei stained for p53. When the surface of the cell membrane was clearly stained for Her2/*neu*, the staining was categorized as strongly positive (2+), while faint staining (in which the difference between the membrane and the cytoplasm was often unclear) was rated weakly positive (1+). ER and PgR status was determined by immunohistochemistry using an automated stainer ("BenchMark" system, Ventana Medical Systems, Tucson, AR), and was judged positive when more than 10% of the cancer cell nuclei were immunoreactive.²⁸⁾

Statistical analysis. The correlation between the patients' clinicopathologic and biological markers and the presence of CK 8/18 degradation products was analyzed by the χ^2 test. A *P* value <0.05 was considered to indicate statistical significance.

Results

1-D immunoblot analysis. The Ub-conjugated proteins found in cancerous and normal tissues from the same breast cancer specimen were compared by 1-D immunoblot analysis (Fig. 1). Extracts from 25 of the 50 (50%) cancerous tissue specimens yielded Ub-immunoreactive bands at about 43 kDa. These were detected by both anti-Ub mAbs (KM680 and KM691), were clearly visible as a single broad band or as double bands, and were derived only from the protein extracts of the cancerous tissues. Normal tissue extracts yielded no bands in the 43-kDa region.

Table 1 shows the correlation between clinicopathologic and biological factors and Ub-immunoreaction at 43 kDa in 50 breast cancer cases. Significant differences in the percentages of cancerous tissues with immunoreaction at 43 kDa were noted according to histologic grade (*P*=0.011): immunoreaction at 43 kDa was detected in one (20%) of five Grade 1 cancers, six (33%) of 18 Grade 2 cancers, and 18 (67%) of 27 Grade 3 cancers. Accumulation of p53 protein in the nuclei (*P*=0.015) and overexpression of Her2/*neu* protein (*P*=0.012) were more frequent in cancerous tissues with immunoreaction at 43 kDa than in those without. No other clinicopathologic factors were correlated with immunoreaction at 43 kDa.

Other bands detected in extracts from cancer tissue were seen at about 100 kDa in 27 cases (54%), whereas 14 (28%) normal tissues yielded low-molecular-weight bands. Neither the 100-

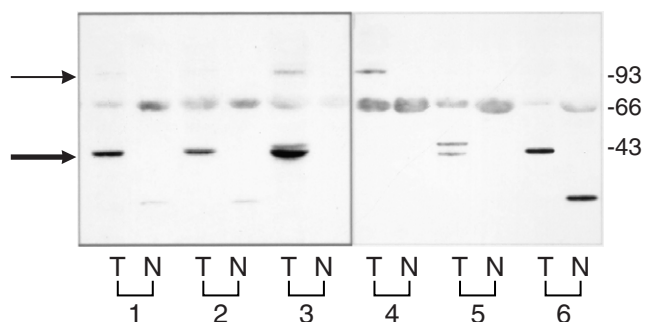


Fig. 1. Profiles of Ub-immunoreactive proteins in breast cancer tissue compared with normal tissues. The case numbers are shown at the bottom of each lane. Extracts of breast cancer tissue (T) and normal breast tissue (N) from the same specimen were loaded on 10% polyacrylamide gel. The anti-Ub antibodies KM691 and KM680 detected immunoreaction bands at about 43 kDa (thick arrow) and 100 kDa (thin arrow) in some tumor tissue. Normal tissue yielded low-molecular-weight immunoreaction bands (cases 1, 2 and 6). Amino acid analysis confirmed the 66-kDa band of immunoreaction with anti-Ub antibody to be serum albumin, which is known to be a ubiquitinated protein.

kDa band nor the low-molecular-weight band was correlated with clinicopathologic factors, expression of p53 protein, or expression of Her2/*neu* protein.

2-D electrophoresis, and immunoblot analysis. The constituents of the 43-kDa bands from the immunoreactive specimens were further analyzed by 2-D electrophoretic separation. Fig. 2 shows two cancerous specimens, which produced a highly concentrated pattern of spots between 40 kDa and 45 kDa. These spots were similar in shape and isoelectric shift, and immunoreacted strongly with the anti-Ub mAbs. This profile of continuous spots was found in cancerous tissue, but not in normal tissue, after CuCl₂ staining. Similar results were obtained with cancer tissue extracts from another 16 specimens that yielded 43-kDa bands on 1-D PAGE.

Sequencing and mass spectrometric analysis. Four distinct spots showing a strongly positive immunoreaction for Ub were selected for further characterization from among the protein spots separated on the 2-D gel. These spots (numbered in Fig. 2) were cut from about five 2-D gels, and the purified proteins were analyzed by partial amino acid sequencing and mass spectrometry. A total of 315 residues were investigated, and the partial amino acid sequencing data are shown in Figs. 3 and 4. Spots 1 and 3 showed 100% homology with CK8, while spots 2 and 4 showed 100% homology with CK18. Their identification was confirmed by the fact that the molecular weights of the partial peptides obtained by mass spectrometry corresponded to those of CK8 and 18 as cut by *Achromobacter* protease I. None of the sequences of any of the digested peptides determined by mass analysis included the N-terminal region of either of the CK proteins. This finding was consistent with the fact that the CK8 and CK18 spots on the 2-D gel had lower molecular weights than their intact counterparts. The spots were therefore

Table 1. Correlation between clinicopathologic and biologic factors and Ub-immunoreaction at 43 kDa in 50 breast cancer specimens

	No. of patients	Ub-immunoreaction at 43 kDa	<i>P</i> value
Tumor size (cm)			
<2	25	12 (48%)	0.812
2-5	14	8 (57%)	
>5	11	5 (45%)	
Number of metastatic lymph nodes			
0	21	8 (38%)	0.354
1-3	15	9 (60%)	
>4	14	8 (57%)	
Histologic grade			
Grade 1	5	1 (20%)	0.011
Grade 2	18	6 (33%)	
Grade 3	27	18 (67%)	
ER status			
Positive	40	18 (45%)	0.157
Negative	10	7 (70%)	
PgR status			
Positive	35	15 (43%)	0.123
Negative	15	10 (67%)	
Nuclear accumulation of p53 protein			
Positive	16	12 (75%)	0.015
Negative	34	13 (38%)	
Overexpression of Her2/ <i>neu</i> protein			
Negative	36	14 (39%)	0.012
1+	7	6 (86%)	
2+	7	5 (71%)	

ER, estrogen receptor; PgR, progesterone receptor.

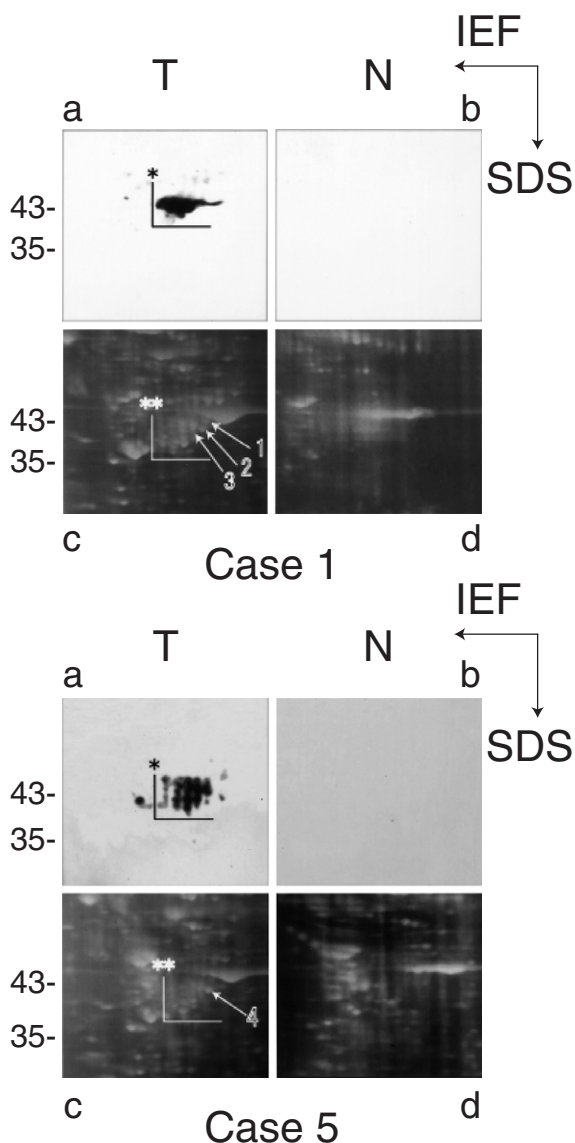


Fig. 2. Profiles of Ub-immunoreactive proteins on 2-D gels from cases 1 and 5. 2-D PAGE immunoblot with anti-Ub mAb and corresponding 2% CuCl_2 staining were performed in 43-kDa immunoreaction-positive cases (cases 1 and 5 in Fig. 1). The 43-kDa immunoreaction bands were composed of several immunoreactive spots whose molecular weights gradually decreased within the 40–45 kDa range framed in (*) in the cancer tissue (T, a). A corresponding group of several spots is indicated by (**) in the CuCl_2 -stained gel (T, c). No immunoreactive spot or corresponding protein spot was detected in the normal tissue (N, b and d).

considered to be degradation products rather than the complete proteins. Similarly, 10 spots from cancer tissue extracts of five other specimens that yielded anti-Ub mAb-immunoreactive products at 40–45 kDa were compared with the HPLC map of the peptides digested by *Achromobacter* protease I. Six of these spots showed a pattern typical of CK18 fragments, while the remaining four were typical of CK8 fragments.

Immunoprecipitation of Ub-immunoreactive CK8/18 in breast cancer tissue. Immunoprecipitation by anti-Ub rabbit polyclonal antibody was performed in cancer and normal tissues of breast cancer specimens. A distinct band was detected by anti-CK18 mouse monoclonal antibody in the precipitated sample of breast cancer tissue (lane T of Fig. 5a). But no band was detected in that of normal tissue (lane N of Fig. 5a). Extracts from breast cancer and normal tissue were immunoprecipitated by anti-

CK8/18 polyclonal antibody. Ub-immunoreactive band was detected by KM691 in the precipitated sample from cancer tissue (lane T of Fig. 5b), but no band was detected in lane N.

Confocal microscopy of CK18. Confocal microscopy was used to determine the intracellular localization of CK18 in 15 breast cancer specimens, 10 of which had CK8/18 ubiquitinated spots and five of which did not. As shown in Fig. 6A, a frame-like network of filaments was observed in the cytoplasm of the breast cancers that yielded no ubiquitinated CK8/18 spots, whereas in those that did yield ubiquitinated CK8/18 spots, no such network was seen and immunofluorescence was diffusely distributed in the cytoplasm (Fig. 6B).

Discussion

Our results demonstrate the expression of lower molecular weight forms of CK proteins in human breast cancer tissue. We analyzed 14 protein spots by partial amino acid analysis after digestion by *Achromobacter* protease I and found them to represent two CKs: CK8 and CK18. Because the total amino acid sequences of these spots were not investigated, it is possible that they might actually be mutant forms of CKs or new proteins. However, the molecular weights of the spots diminished gradually, and the two sets of paired spots (spots 1 and 3, and spots 2 and 4) were identified as the same proteins, strongly suggesting that the spots examined corresponded to degraded proteins. Moreover, since all the spots reacted with anti-Ub mAbs and Ub-immunoreactive CKs were immunoprecipitated by anti-CK8/18 antibody, we believe that this degradation is mediated by the Ub-dependent proteasome pathway. To our knowledge, this study is the first to demonstrate *in vivo* a Ub-associated degradation form of CK8/18 in breast cancer tissue.

No Ub-immunoreactive degradation form of CK8/18 was detected in normal breast tissue during this study. One possible reason for the failure to detect Ub-immunoreactive CK in normal tissue is that the amounts of Ub-immunoreactive CKs present were below the sensitivity limit for finding foci on the 2-D gel. Another possibility is that CK8/18 was degraded by other pathways, including caspase-mediated digestion²⁹; however, the reason for the existence of two or more CK degradation pathways is not clear. Nevertheless, we suggest that the major degradation route for CK 8/18 in breast cancer tissue is the Ub-dependent pathway.³⁰ Normal breast tissue is mainly composed of epithelial cells, myoepithelial cells, fibroblasts and adipose cells. Since no Ub-dependent degradation of CKs was detected in these normal cells, we believe that the major changes in cytoskeletal degeneration produced by the Ub-mediated degradation system occur only in cancer cells.

Proteolysis of CKs has previously been observed in several transformed cell lines. Chen *et al.* discovered that adenovirus infection induced a proteolytic product of CK18 in infected HeLa cells.³¹ Immunological examinations of the pattern of keratin expression in a human breast epithelial cell line transfected with a mutated *c-Ha-ras* oncogene showed a decrease in the number of phosphorylated and lower molecular weight forms of CKs,^{32,33} while in an *in vivo* study of human colon cancer tissue, Nishibori *et al.* identified ubiquitinated CK8 fragments.²⁴ Since CK proteolysis was observed only after various gene alterations had been introduced during these studies, changes in the expression of certain genes may induce dynamic degradation and reorganization of CKs.

In normal breast tissue, it is possible to distinguish between basal (or myoepithelial) cells and luminal cells on the basis of their keratin expression patterns. Myoepithelial cells are restricted to the expression of CK5/6, CK14 and CK17, whereas luminal cells express CK7, CK8, CK18 and CK19.³⁴ The keratin expression profile can also be used to subclassify breast carcinomas into basal and luminal cell types.³⁵ The majority of

1	MSIRVTQKSY	KVSTSGPRAF	SSRSYTSQPG	SRISSSSFSR	VGSSNFRGGL
51	GGGYGGASGM	GGITAVTVNQ	SLLSPLSLEV	DPNIGAVRTQ	EKEQIKITLNN
101	<u>KFASFDKVR</u>	<u>FLEQQNKMLE</u>	<u>TKWSLLQQQK</u>	TARSNMDNMF	ESYINNLRRQ
151	LETLGQEKLK	LEAELGNMQG	LYEDFKNKYE	DEINKRTEME	NEFVLIKDDV
201	<u>DEAYMNKVEL</u>	ESRLEGLTDE	INFLRQLYEE	EIRELQSQIS	DTSVVLSDMN
251	SRSLDMDSII	AEVKAQYEDI	<u>ANRSRAEAEES</u>	<u>MYQIKYEELQ</u>	<u>SLAGKHGDDL</u>
301	<u>RRTKTEISEM</u>	<u>NRNISRLQAE</u>	<u>IEGLKGQRAS</u>	<u>LEAAIADAEQ</u>	<u>RGELAIKDAN</u>
351	<u>AKLSELEAAL</u>	<u>QRAKQDMARG</u>	LREYQELMNV	<u>KLALDIEIAT</u>	<u>YRKLEGEES</u>
401	<u>RLESGMQNMS</u>	<u>IHTKTTGGYA</u>	GGLSSAYGDL	TDPGLSYSLG	SSFSGSAGSS
451	SFSRTSSSRA	VVVKKIETRD	GKLVSESSDV	LPK	

Fig. 3. Amino acid sequence of spot 1 (corresponding to CK8). The protein eluted from spot 1 in Fig. 2 was examined by partial amino acid sequencing. The amino acid residues investigated are underlined. The sequence corresponds to that of CK8 (100% homology). Spot 3 corresponds to the same protein.

1	MSFTTRSTFS	TNYRSLGVSQ	APSYGARPVS	SAASVYAGAG	GSGSRISVSR
51	STSFRRGGMGS	GGLATGIAGG	LAGMGGIQNE	KETMQSLNDR	LASYLDRVRS
101	LETENRRLES	KIREHLEKKG	PQVRDWSHYF	KIIEDLRAQI	FANTVDNARI
151	VLQIDNARLA	ADDFRVKYET	ELAMRQSVEN	DIHGLRKVID	DTNITRLQLE
201	TEIEALKEEL	LFMKNHEEE	<u>VKGLQAQIAS</u>	<u>SGLTVEVDAP</u>	<u>KSQDLAKIMA</u>
251	<u>DIRAQYDELA</u>	<u>RKNREELDKY</u>	<u>WSQQIEESTT</u>	<u>VVTTQSAEVG</u>	<u>AAETTLTELR</u>
301	RTVQSLEIDL	DSMRNLKASL	ENSLREVEAR	YALQMEQLNG	ILLHLESELA
351	QTRAEGRQA	QEYEALLNIK	VKLEAEIATY	RRLLEDGEDF	NLGDALDSSN
401	<u>SMQTIQKITT</u>	<u>RRIVDGKVVS</u>	ETNDTKVLRH		

Fig. 4. Amino acid sequence of spot 2 (corresponding to CK18). The protein eluted from spot 2 in Fig. 2 was examined by partial amino acid sequencing. The amino acid residues investigated are underlined. The sequence corresponds to that of CK18 (100% homology). Spot 4 corresponds to the same protein.

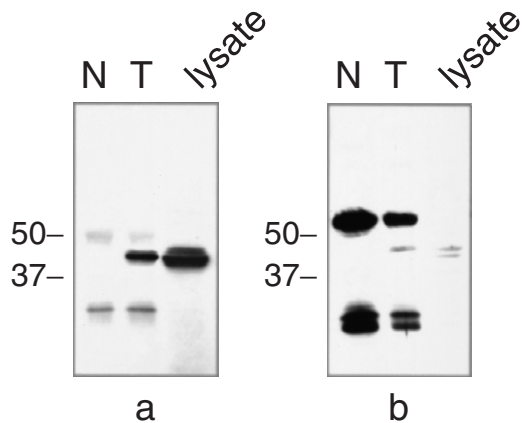


Fig. 5. Immunoprecipitation of Ub-immunoreactive CK8/18. a. Extracts from normal and breast cancer tissue of the same specimen were immunoprecipitated by anti-Ub rabbit polyclonal antibody. The Ub-immunoreactive CK18 was detected by anti-CK18 mouse monoclonal antibody in the precipitated sample from breast cancer tissue (lane T). No band was detected in that of normal tissue (lane N). The lane of lysate showed the result of immunoblot analysis with anti-CK18 antibody of breast cancer tissue. b. Extracts from normal and cancer tissue of breast cancer specimen were precipitated with anti-CK8/18 polyclonal antibody. Lane T shows the Ub-immunoreactive band detected by KM691 in the precipitated sample from cancer tissue (T); no band was detected in lane N. The lane of lysate shows the result of immunoblot analysis by KM691 in breast cancer tissue.

breast cancers with high histological grade express CKs 4, 14 and/or 17 and this expression pattern (basal cell type) is associated with shorter disease-free survival in node-positive breast carcinomas.³⁶⁾ To the contrary, an immunohistochemical study revealed that a high CK18 expression level is a strong indicator of a favorable prognosis.³⁷⁾ A recent examination of gene expression patterns using microarray analysis showed that breast cancer can be subclassified into basal or luminal types.³⁸⁾ The expression pattern of the basal type, which shows a low level of CK8/18 mRNA expression, is significantly associated with a

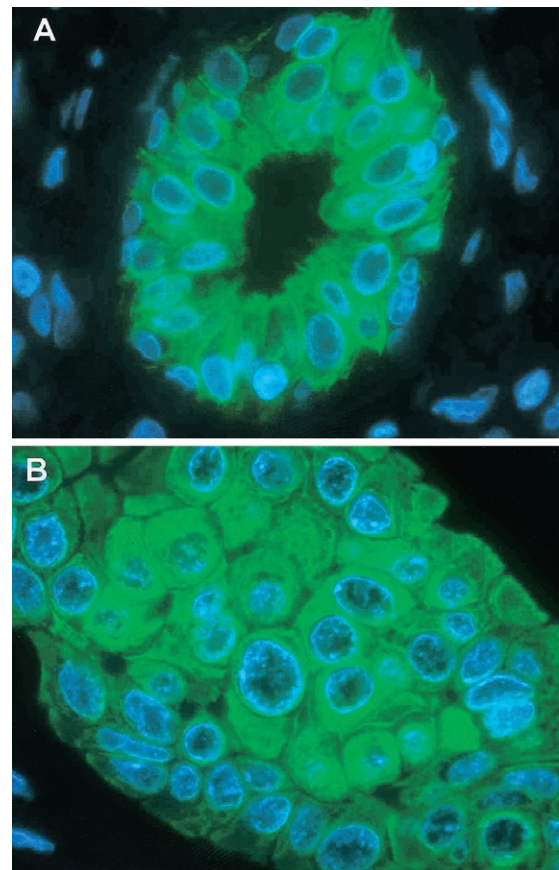


Fig. 6. Intracellular localization of CK18 in breast cancer cells as revealed by confocal microscopy. A. An intracytoplasmic network of filaments was detected close to the membrane in breast cancer cells that did not yield Ub-immunoreactive CK8/18 spots on 2-D PAGE. B. Diffuse staining for CK18 was present, but no network structure was detected, in the cytoplasm of breast cancer cells that yielded Ub-immunoreactive CK8/18 spots.

poor outcome³⁹); this finding was confirmed by an immunohistochemical study using 600 breast tumors.⁴⁰ Dynamic changes in the expression pattern occur at the mRNA level during the progression of breast cancer, and the protein expression pattern changes in parallel. Accordingly, the degradation of the majority of CK8/18 via a Ub-dependent pathway, as observed during the present study, may explain why breast cancer cells exhibit a basal-type expression pattern at the protein level.

Our sequencing data showed that Ub-immunoreactive CK18 does not have the N-terminal residue of CK18, suggesting deletion of the N-terminal residue of CK18. However, our data could not exclude the possibility that digested peptides of the N-terminal region are still attached to the PVDF membrane. However, visualization of the intracytoplasmic distribution of CK18 in the breast cancer cells showed that filament organization was lost in cancerous tissue with fragmented CKs. These findings are consistent with loss of the N-terminal residue of CK18, because the N-terminal region is very important for filament organization.⁴¹ Disruption of the CK system would weaken the mechanical integrity of the cell, and this could in part explain some of the morphologic alterations observed in breast cancer. Moreover, CKs are highly dynamic proteins that reorganize during various cellular events, such as mitosis and apoptosis.^{42,43} Clinically aggressive breast cancer has been associated with nuclear accumulation of p53, overexpression of Her2/*neu* and a high histologic grade. Because the Ub-immunoreactive degradation products of CKs were correlated with these three characteristics during the present study, it is highly likely that loss of CKs, or impairment of their function, due to cancer-specific degradation is an important factor in enhancing the aggressiveness of breast cancer.

Although CK8/18 is known to be degraded in a Ub-dependent manner,³⁰ we did not directly confirm that CK8/18 was

degraded in the breast cancer tissue. Our data showed that fragmented CK8/18 was immunoreactive for Ub in breast cancer tissue. Fragmented CK8/18 may be stable and have an important role in facilitating aggressive clinical behavior of breast cancer. Another possibility is that Ub-dependent degradation is disturbed in cancer cells. To clarify the meaning of the existence of fragmented CK8/18 in breast cancer cells, examination of Ub-immunoreactive CK8/18 fragments themselves is necessary. Moreover, direct mass spectrometric analysis of Ub-immunoreactive CK8/18 fragments should be done. Ub was not detected by sequencing or mass spectrometric analysis. Ub is known to be hardly digested by *Achromobacter* protease I. We think that Ubs were possibly undigested and remained on the PVDF membrane. A better knowledge of the ubiquitination of CK8/18 should be the key to understanding the role of Ub-immunoreactive CK8/18 fragments.

In conclusion, breast-cancer-specific spots that reacted with anti-Ub mAbs were detected by 2-D electrophoresis and identified as degraded forms of CK8/18. The presence of these abnormal CKs was associated with an aggressive morphology, overexpression of Her2/*neu* protein and nuclear accumulation of p53. Though further study is necessary to determine directly whether complete degradation of CKs occurs via a Ub-dependent proteasome pathway, these findings suggest that the degradation is an important step in inducing the protein expression pattern of aggressive breast cancer.

The authors are grateful to Mr. Seiji Sato and Mr. Hiroaki Kono, Kyowa Hakko Kogyo Co., Ltd., for providing the anti-Ub mAbs. This study was supported in part by Grants in Aid for Cancer Research and for the 2nd Term Comprehensive Strategy for Cancer Control from the Ministry of Health, Labour and Welfare, Japan.

- Ozkaynak E, Finley D, Varshavsky A. The yeast ubiquitin gene: head-to-tail repeats encoding a polyubiquitin precursor protein. *Nature* 1984; **312**: 663–6.
- Hershko A, Ciechanover A, Varshavsky A. Basic Medical Research Award. The ubiquitin system. *Nat Med* 2000; **6**: 1073–81.
- Hershko A, Leshinsky E, Ganoth D, Heller H. ATP-dependent degradation of ubiquitin-protein conjugates. *Proc Natl Acad Sci USA* 1984; **81**: 1619–23.
- Bachmair A, Varshavsky A. The degradation signal in a short-lived protein. *Cell* 1989; **56**: 1019–32.
- Ciechanover A, Orian A, Schwartz AL. Ubiquitin-mediated proteolysis: biological regulation via destruction. *Bioassays* 2000; **22**: 442–51.
- Iwai K, Yamanaka K, Kamura T, Minato N, Conaway RC, Conaway JW, Klausner RD, Pause A. Identification of the von Hippel-Lindau tumor-suppressor protein as part of an active E3 ubiquitin ligase complex. *Proc Natl Acad Sci USA* 1999; **96**: 12436–41.
- Ishibashi Y, Takada K, Joh K, Ohkawa K, Aoki T, Matsuda M. Ubiquitin immunoreactivity in human malignant tumours. *Br J Cancer* 1991; **63**: 320–2.
- Osada T, Sakamoto M, Nishibori H, Iwaya K, Matsuno Y, Muto T, Hirohashi S. Increased ubiquitin immunoreactivity in hepatocellular carcinomas and precancerous lesions of the liver. *J Hepatol* 1997; **26**: 1266–73.
- Kern SE, Kinzler KW, Bruskin A, Jarosz D, Friedman P, Prives C, Vogelstein B. Identification of p53 as a sequence-specific DNA-binding protein. *Science* 1991; **252**: 1708–11.
- Lowe SW, Ruley HE, Jacks T, Housman DE. p53-dependent apoptosis modulates the cytotoxicity of anticancer agents. *Cell* 1993; **74**: 957–67.
- el-Deiry WS, Tokino T, Velculescu VE, Levy DB, Parsons R, Trent JM, Lin D, Mercer WE, Kinzler KW, Vogelstein B. WAF1, a potential mediator of p53 tumor suppression. *Cell* 1993; **75**: 817–25.
- Ries S, Biederer C, Woods D, Shifman O, Shirasawa S, Sasazuki T, McMahon M, Oren M, McCormick F. Opposing effects of Ras on p53: transcriptional activation of mdm2 and induction of p19ARF. *Cell* 2000; **103**: 321–30.
- Iwaya K, Tsuda H, Hiraide H, Tamaki K, Tamakuma S, Fukutomi T, Mukai K, Hirohashi S. Nuclear p53 immunoreaction associated with poor prognosis of breast cancer. *Jpn J Cancer Res* 1991; **82**: 835–40.
- Friedrichs K, Gluba S, Eidtmann H, Jonat W. Overexpression of p53 and prognosis in breast cancer. *Cancer* 1993; **72**: 3641–7.
- Rosen PP, Lesser ML, Arroyo CD, Cranor M, Borgen P, Norton L. p53 in node-negative breast carcinoma: an immunohistochemical study of epidemiologic risk factors, histologic features, and prognosis. *J Clin Oncol* 1995; **13**: 821–30.
- Iwaya K, Tsuda H, Fukutomi T, Tsugane S, Suzuki M, Hirohashi S. Histologic grade and p53 immunoreaction as indicators of early recurrence of node-negative breast cancer. *Jpn J Clin Oncol* 1997; **27**: 6–12.
- Iwaya K, Tsuda H, Fujita S, Suzuki M, Hirohashi S. Natural state of mutant p53 protein and heat shock protein 70 in breast cancer tissues. *Lab Invest* 1995; **72**: 707–14.
- Band V, De Caprio JA, Delmolino L, Kulesa V, Sager R. Loss of p53 protein in human papillomavirus type 16 E6-immortalized human mammary epithelial cells. *J Virol* 1991; **65**: 6671–6.
- Haupt Y, Maya R, Kazaz A, Oren M. Mdm2 promotes the rapid degradation of p53. *Nature* 1997; **387**: 296–9.
- Sato Y, Mukai K, Watanabe S, Goto M, Shimosato Y. The AMeX method. A simplified technique of tissue processing and paraffin embedding with improved preservation of antigens for immunostaining. *Am J Pathol* 1986; **125**: 431–5.
- Elston CW, Ellis IO. Pathological prognostic factors in breast cancer. I. The value of histological grade in breast cancer: experience from a large study with long-term follow-up. *Histopathology* 1991; **19**: 403–10.
- Bradford MM. A rapid and sensitive method for the quantitation of microgram quantities of protein utilizing the principle of protein-dye binding. *Anal Biochem* 1976; **72**: 248–54.
- Kanayama H, Tanaka K, Aki M, Kagawa S, Miyaji H, Satoh M, Okada F, Sato S, Shimbara N, Ichihara A. Changes in expressions of proteasome and ubiquitin genes in human renal cancer cells. *Cancer Res* 1991; **51**: 6677–85.
- Nishibori H, Matsuno Y, Iwaya K, Osada T, Kubomura N, Iwamatsu A, Kohno H, Sato S, Kitajima M, Hirohashi S. Human colorectal carcinomas specifically accumulate Mr 42,000 ubiquitin-conjugated cytokeratin 8 fragments. *Cancer Res* 1996; **56**: 2752–7.
- Iwamatsu A. S-Carboxymethylation of proteins transferred onto polyvinylidene difluoride membranes followed by *in situ* protease digestion and amino acid microsequencing. *Electrophoresis* 1992; **13**: 142–7.
- Aebbersold RH, Leavitt J, Saavedra RA, Hood LE, Kent SB. Internal amino acid sequence analysis of proteins separated by one- or two-dimensional gel electrophoresis after *in situ* protease digestion on nitrocellulose. *Proc Natl Acad Sci USA* 1987; **84**: 6970–4.
- Henzel WJ, Billeci TM, Stults JT, Wong SC, Grimley C, Watanabe C. Identifying proteins from two-dimensional gels by molecular mass searching of

- peptide fragments in protein sequence databases. *Proc Natl Acad Sci USA* 1993; **90**: 5011–5.
28. Goldhirsch A, Glick JH, Gelber RD, Senn HJ. Meeting highlights: International Consensus Panel on the Treatment of Primary Breast Cancer. *J Natl Cancer Inst* 1998; **90**: 1601–8.
 29. Caulin C, Salvesen GS, Oshima RG. Caspase cleavage of keratin 18 and reorganization of intermediate filaments during epithelial cell apoptosis. *J Cell Biol* 1997; **138**: 1379–94.
 30. Ku NO, Omary MB. Keratins turn over by ubiquitination in a phosphorylation modulated fashion. *J Cell Biol* 2000; **149**: 547–52.
 31. Chen PH, Ornelles DA, Shenk T. The adenovirus L3 23-kilodalton proteinase cleaves the amino-terminal head domain from cytokeratin 18 and disrupts the cytokeratin network of HeLa cells. *J Virol* 1993; **67**: 3507–14.
 32. Breitkreutz D, Boukamp P, Ryle CM, Stark HJ, Roop DR, Fusenig NE. Epidermal morphogenesis and keratin expression in c-Ha-ras-transfected tumorigenic clones of the human HaCaT cell line. *Cancer Res* 1991; **51**: 4402–9.
 33. Paine TM, Fontanini G, Basolo F, Geronimo I, Elliott JW, Russo J. Mutated c-Ha-ras oncogene alters cytokeratin expression in the human breast epithelial cell line MCF-10A. *Am J Pathol* 1992; **140**: 1483–8.
 34. Dairkee S, Heid HW. Cytokeratin profile of immunomagnetically separated epithelial subsets of the human mammary gland. *In Vitro Cell Dev Biol Anim* 1993; **29A**: 427–32.
 35. Dairkee SH, Puett L, Hackett AJ. Expression of basal and luminal epithelium-specific keratins in normal, benign, and malignant breast tissue. *J Natl Cancer Inst* 1988; **80**: 691–5.
 36. Malzahn K, Mitze M, Thoenes M, Moll R. Biological and prognostic significance of stratified epithelial cytokeratins in infiltrating ductal breast carcinomas. *Virchows Arch* 1998; **433**: 119–29.
 37. Schaller G, Fuchs I, Pritze W, Ebert A, Herbst H, Pantel K, Weitzel H, Lengyel E. Elevated keratin 18 protein expression indicates a favorable prognosis in patients with breast cancer. *Clin Cancer Res* 1996; **2**: 1879–85.
 38. Perou CM, Sorlie T, Eisen MB, van de Rijn M, Jeffrey SS, Rees CA, Pollack JR, Ross DT, Johnsen H, Akslen LA, Fluge O, Pergamenschikov A, Williams C, Zhu SX, Lonning PE, Borresen-Dale AL, Brown PO, Botstein D. Molecular portraits of human breast tumours. *Nature* 2000; **406**: 747–52.
 39. Sorlie T, Perou CM, Tibshirani R, Aas T, Geisler S, Johnsen H, Hastie T, Eisen MB, van de Rijn M, Jeffrey SS, Thorsen T, Quist H, Matese JC, Brown PO, Botstein D, Eystein Lonning P, Borresen-Dale AL. Gene expression patterns of breast carcinomas distinguish tumor subclasses with clinical implications. *Proc Natl Acad Sci USA* 2001; **98**: 10869–74.
 40. van de Rijn M, Perou CM, Tibshirani R, Haas P, Kallioniemi O, Kononen J, Torhorst J, Sauter G, Zuber M, Kochli OR, Mross F, Dieterich H, Seitz R, Ross D, Botstein D, Brown P. Expression of cytokeratin 17 and 5 identifies a group of breast carcinomas with poor clinical outcome. *Am J Pathol* 2002; **161**: 1991–6.
 41. Bader BL, Magin TM, Freudenmann M, Stumpp S, Franke WW. Intermediate filaments formed *de novo* from tail-less cytokeratins in the cytoplasm and in the nucleus. *J Cell Biol* 1991; **115**: 1293–307.
 42. Franke WW, Schmid E, Wellsteed J, Grund C, Gigi O, Geiger B. Change of cytokeratin filament organization during the cell cycle: selective masking of an immunologic determinant in interphase PtK2 cells. *J Cell Biol* 1983; **97**: 1255–60.
 43. Leers MP, Kolgen W, Bjorklund V, Bergman T, Tribbick G, Persson B, Bjorklund P, Ramaekers FC, Bjorklund B, Nap M, Jornvall H, Schutte B. Immunocytochemical detection and mapping of a cytokeratin 18 neo-epitope exposed during early apoptosis. *J Pathol* 1999; **187**: 567–72.